



## ARTICLE IN PRESS



ELSEVIER

Available at  
www.ComputerScienceWeb.com  
POWERED BY SCIENCE @ DIRECT®

NEUROCOMPUTING

Neurocomputing III (IIII) III-III

www.elsevier.com/locate/neucom

1

3

5

7

# Realtime bioelectrical data acquisition and processing from 128 channels utilizing the wavelet-transformation<sup>☆</sup>

Andre Folkers\*, Florian Mösch, Thomas Malina,  
Ulrich G. Hofmann

*Institute for Signal Processing, University of Lübeck, Germany*

---

### Abstract

9 We propose a versatile signal processing and analysis framework for bioelectrical data, and in particular for neural recordings and EEG. Within this framework the signal is decomposed into subbands using fast wavelet transform algorithms, executed in real-time on a current digital signal processors hardware platform. The decomposition is used to perform various processing and analysis tasks. Besides fast implementation of high, band, low pass filters, the decomposition is used for denoising and lossy, as well as lossless compression. Furthermore specific electrophysiological analysis tasks like spike detection and sorting are performed within this decomposition scheme.

17 © 2002 Published by Elsevier Science B.V.

*Keywords:* Digital signal processor; Data acquisition; Spike detection; Wavelet transformation

---

### 19 1. Overview

21 Recording neural activity from a high number of neurons is a key issue in understanding how the brain works. Within the project VSAMUEL we developed successfully a versatile data acquisition system based on DSP boards [3]. The system is used for continuous neural data acquisition in vivo or in vitro with a high channel count (up to 128 channels) at sampling rate  $F = 50$  kHz with a precision of 16 bits per sample.

---

<sup>☆</sup> This work has been supported by EU grant IST-1999-10073.

\* Corresponding author. Medical University of Luebeck, Seelandstr 1a Geb. 5, Luebeck 23569, Germany. Fax: +49-451-3909-555.

*E-mail address:* folkers@isip.mu-luebeck.de (A. Folkers).

1 Important online data processing tasks include filtering and spike detection and classifi-  
 2 cation, but also compression, transmission and storage. We propose a signal processing  
 3 framework within which these tasks can be performed in an elegant way.

2. Wavelet transform and lifting scheme

5 The signal is decomposed into  $N + 1$  subbands by a  $N$ -level wavelet transform  
 6 (WT). The subbands  $d_j, j = 1, \dots, N$  represent the frequency band  $[F/2^{j+1}, F/2^{j+2}]$   
 7 and the subband  $a_N$  represents  $[0, F/2^{N+1}]$ . Fig. 1 shows the filter bank for  $N = 3$ . In each  
 8 step the signal is decomposed by applying complementary filters to  $a_j$ , i.e. a high  
 9 pass  $\tilde{g}$  and a low pass  $\tilde{h}$ , which are determined by the selected wavelet. The results of  
 10 both filter operations are subsampled by a factor of two, leading to subbands  $d_{j+1}$   
 11 and  $a_{j+1}$ . Note, that the number of coefficients in  $d_{j+1}$  and  $a_{j+1}$  is equal to the number  
 12 of coefficients in  $a_j$ . The wavelet transform is implemented using the lifting scheme  
 13 which is faster than the standard implementation (Fig. 1). It is done in-place, and with  
 14 a small modification it implements a WT that maps integers onto integers [1] while  
 15 preserving the possibility of perfect reconstruction. Therefore, this implementation of  
 16 the WT is well suited for realtime processing using digital signal processors (DSP).

17 The lifting scheme provides another point of view to the wavelet transform. Basically  
 18 it consists of three stages, which are a *split*, a *predict*, and an *update* stage as illustrated  
 19 in Fig. 2 [6]. First the signal is split such that we obtain two sequences  $d_j$  and  $a_j$  which  
 20 in our case consist of sample points with odd and with even indices, respectively. Now,  
 21

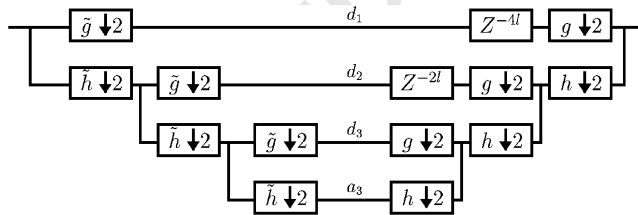


Fig. 1. Filter bank with three levels.

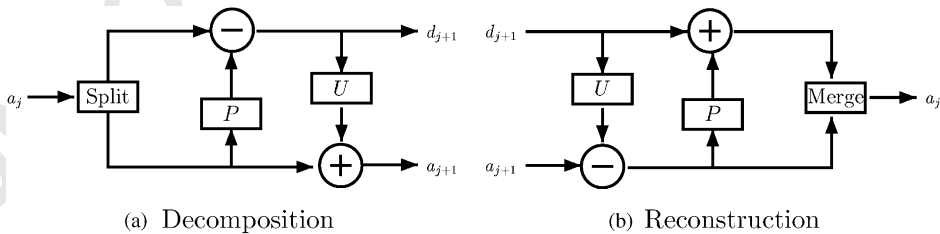


Fig. 2. Basic structure of the lifting scheme: (a) decomposition, and (b) reconstruction.

1 we predict the values in  $d_j$  based on  $a_j$  as  $P(a_j)$ . Under the assumption that the  
2 signal is continuous we have a good chance that our prediction is rather close to the  
3 actual values. We compute the difference between prediction and actual values, and  
4 keep these values which are likely to be small:  $d_{j+1} = d_{j+1} - P(a_{j+1})$ . In order to  
5 preserve certain properties of the original signal in the coefficients  $a_j$ , e.g. the mean  
6 value, we need the third stage, which is the update stage. Hereby, the values in  $a_j$   
7 are modified by using an appropriate update operator on values in  $d_j$  and  $U(d_j)$ :  
8  $a_{j+1} = a_{j+1} + U(d_{j+1})$ .

9 The perfect reconstruction property of the lifting scheme is obvious, because we can  
10 obtain  $a_j$  from  $a_{j+1}$  and  $d_{j+1}$  by inverting the data flow and the signs as shown in Fig.  
11 2(b). Note, that this holds for arbitrary predict and update operators. Therefore, if these  
12 operators include a rounding to the next integer we obtain a wavelet transform that  
13 maps integer onto integers. It is possible to implement arbitrary wavelet transformations  
14 as shown in [1] by using multiple prediction and update operators successively. The  
15 respective operators are computed according to the given mother wavelet.

16 Using the lifting scheme and a routine optimized for our DSP, we can apply a six  
17 level Daubechies 2 decomposition filter bank on 32 channels sampled at 50 kHz in  
18 real time.

### 19 3. Filter

20 The decomposition allows a simple implementation of filters with different high pass,  
21 band pass, or low pass characteristics. Consider, e.g. a neural recording sampled at  
22  $F = 50$  kHz which contains both field potentials and action potentials. If it is decom-  
23 posed by a 6-level WT into 7 subbands, then the field potentials are found in subband  
24  $a_6$ . Setting the coefficients of  $a_6$  to zero, eliminates the field potentials and corresponds  
25 to a high pass filter (Fig. 3). The respective low pass filter which eliminates the action  
26 potentials is obtained by setting the coefficients  $d_j$  for  $j=1, \dots, 6$  to zero. A comparison  
27 of the results of both methods can be found in Fig. 3. Fig. 4 shows a comparison of  
28 the respective frequency responses. The decomposition also allows the implementation  
29 of band pass filters. Possible cut-off frequencies for band pass filter based on the WT  
30 are determined by the sampling rate and the number of levels. Arbitrary filters can be  
31 implemented if a Wavelet Packet Transform (WPT, see [8]) is utilized. However, the  
32 computation of the WPT transform involves more operations than the WT. Because  
33 the number of operations has to be as low as possible to allow real-time computation  
34 on our DSP, we currently restrict ourselves to the WT.

### 35 4. Compression and denoising

36 One important property of the WT is that it decorrelates the signal, i.e. the main  
37 information about the signal is collected in a few large coefficients, while the details  
38 are collected in many small coefficients. The average information content, also called

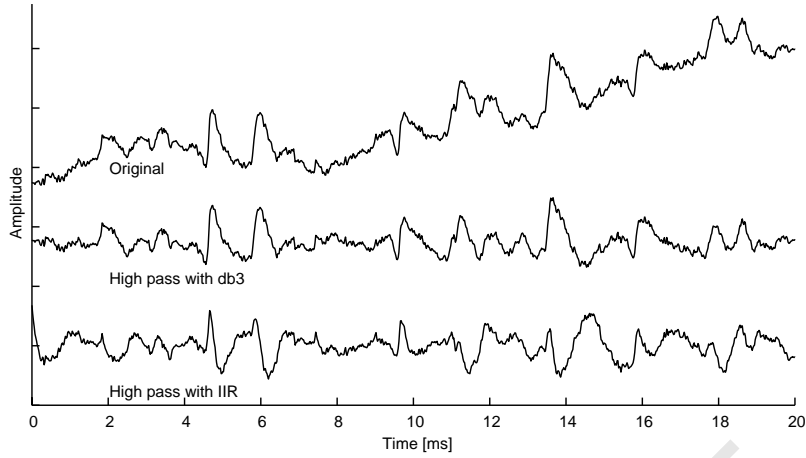


Fig. 3. High pass filtering using IIR versus elimination of wavelet approximation coefficients. The original neural recording has been decomposed with a 6 level WT using the Daubechies 4 wavelet. The coefficients of  $a_6$  have been set to zero, corresponding to a high pass filtering with cut-off at 390.62 Hz. In a second approach the signal has been filtered by a 4-pole IIR high pass filter with cut-off at frequency 400 Hz, which was designed using the Butterworth method. Spike shapes in the IIR filtered result show significant distortions, while the spike shapes are apparently not distorted by the wavelet based high pass. Field potentials are eliminated well by both filters.

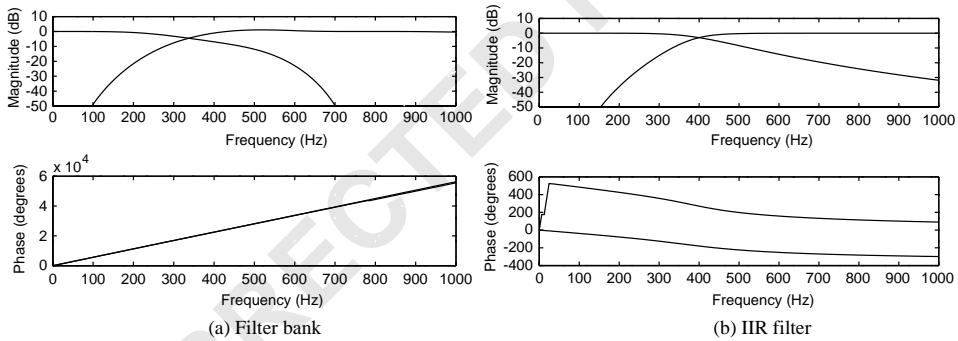


Fig. 4. Comparison of filter bank based (a) and IIR (b) high and low pass filter. For the filter bank Daubechies wavelet with four vanishing moments has been used. The IIR filter have order 4 and cut off frequency at 400 Hz. The magnitudes of the frequency responses are comparable, but the phase of the filter bank is linear while the phase of the IIR filter is nonlinear, which is the reason for the distortions found in Fig. 3.

1 *entropy*, can be computed as

$$E(s) = - \sum_{v \in \text{Values of } s} p(v) \log_2(p(v)), \quad (1)$$

3 where  $p(v)$  is the probability of occurrence of value  $v$  within signal  $s$ . The entropy is measured in bits per sample and since our signals are sampled in 16 bit resolution,

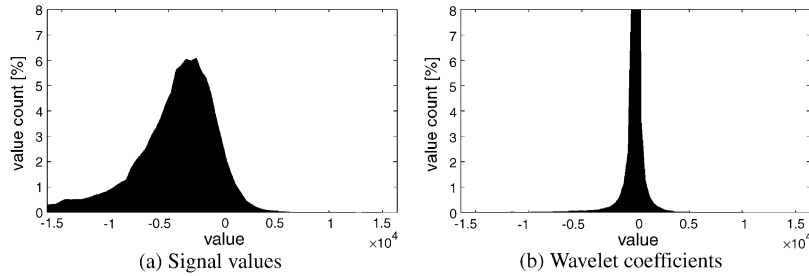


Fig. 5. Entropy reduction by wavelet transformation is illustrated by a comparison of the signal value and the wavelet coefficient histograms: (a) signal values, and (b) wavelet coefficients.

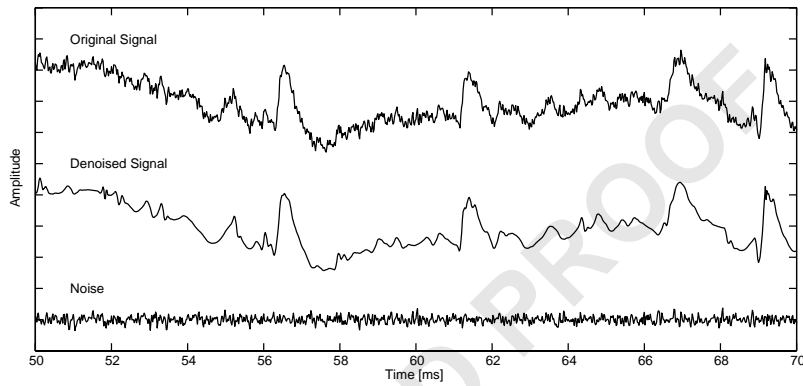


Fig. 6. Compression and denoising. The comparison of the original neural signal at the top and the denoised signal in the middle reveals no apparent distortion of the signal. This is confirmed by the difference of signal and denoised signal, i.e. the removed noise, which is shown at the bottom. The entropy of the decomposition drops from 8.34 bits per sample down to 1.04 bits per coefficient. In other words the compression rate can be improved by a factor of 8.

- 1 we can define the optimal achievable compression rate, e.g. with Huffman coding,
- 2 as  $E(s)/16$ . The entropy of the decomposition is smaller than the entropy of the raw
- 3 signal (Fig. 5). The entropy of a neural recording from a rat was quantified in [7] to be
- 4 about 13.9 bits per sample and it is about 8.5 bits per coefficient for the decomposition.
- 5 Therefore, the compression rate can be improved from 0.86 for the raw data down to
- 6 0.53 for the decomposition.
- 7 Another important task is the denoising of neural recordings. The typical background
- 8 noise of neural recordings is mainly found in the first few levels  $d_1, \dots, d_3$  of the de-
- 9 composition. Under the reasonable assumption that the background noise has a Gaussian
- 10 distribution [5], a universal threshold can be found as  $\delta = \sqrt{2\sigma^2 \log(n)}$  where  $\sigma^2$  is
- 11 the variance of the Gaussian noise and  $n$  is the length of the sequence [2]. Since the
- 12 true variance  $\sigma^2$  is usually unknown, it is estimated from the coefficients in  $d_1$  which
- 13 are dominated by the noise. We use the standard deviation estimator *median absolute*
- 14 *deviation* (MAD):  $\sigma^2 = \text{median}(|d_1|)/0.6745$ . Using the median absolute value instead of

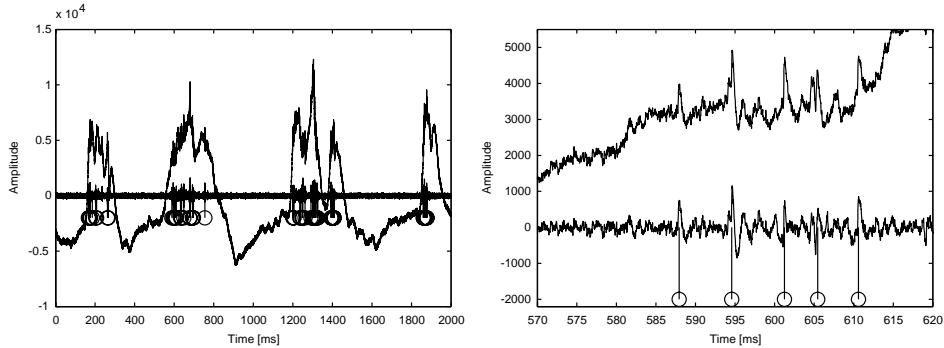


Fig. 7. Spike detection base on wavelet coefficients. Detected spikes are marked by stems. On the right an enlarged section of the signal is shown, which reveals that the signal-to-noise ratio is quite small, but still the spikes are detected well.

- 1 the mean absolute value, this estimation is robust against large coefficients representing
- 2 the signal that might occur in  $d_1$ .
- 3 Compression and denoising are closely related. The thresholded decomposition which
- 4 represents the denoised signal has a much lower entropy than the original decomposition
- 5 and thus can be compressed with a better rate. Depending on the chosen thresholds,
- 6 the compression rate can reach values below 0.1 without losing a significant part of
- 7 the signal. With the universal threshold for instance we obtain a compression rate of
- 8 about 0.06 for neural recordings from a rat (Fig. 6). Lossy compression which does
- 9 not distort the signal significantly is particularly useful for longterm recordings.

## 5. Spike detection

- 11 The decomposition is used to analyse neural recordings. Spikes, for instance, are
- 12 represented by a few large coefficients in subbands  $d_2, \dots, d_6$ . Therefore, spike detection
- 13 can be implemented by a threshold based method which uses the wavelet coefficients.
- 14 In Fig. 7 such a method has been used to detect spike in a neural recording from a rat,
- 15 which contains field potentials and action potentials. In [4] another method to detect
- 16 spikes based on wavelet coefficients is proposed.

## 17 6. Conclusions

- 18 Altogether we can state, that our DAQ system is able to record from a high number
- 19 of channels, and furthermore it can perform sophisticated processing of the incoming
- 20 electrophysiological data in realtime, which in our case is a wavelet decomposition.
- 21 The data obtained from the wavelet decomposition represents the original data without
- 22 loss, and it provides an elegant way to compress and to denoise the signals, and also
- 23 to do further processing, like, e.g. spike detection.

1 **References**

- 3 [1] I. Daubechies, W. Sweldens, Factoring wavelet transforms into lifting steps, *J. Fourier Anal. Appl.* 4 (3) (1998) 245–267.
- 5 [2] D.L. Donoho, I.M. Johnstone, Ideal spatial adaptation by wavelet shrinkage, *Biometrika* 81 (3) (1994) 425–455.
- 7 [3] A. Folkers, U.G. Hofmann, A multichannel data acquisition and analysis system based on off-the-shelf dsp boards, in: *Proceedings of the EURASIP Conference on Digital Signal Processing for Multimedia Communications and Services*, Budapest, September 2001.
- 9 [4] H. Nakatani, T. Watanabe, N. Hoshimiya, Detection of nerve action potentials under low signal-to-noise ratio condition, *IEEE Trans. Biomed. Eng.* 48 (8) (2001) 845–849.
- 11 [5] M. Sahani, Latent variable models for neural data analysis, Ph.D. Thesis, California Institute of Technology, Pasadena, California, 1999.
- 13 [6] W. Sweldens, The lifting scheme: a new philosophy in biorthogonal wavelet constructions, in: A.F. Laine, M. Unser (Eds.), *Wavelet Applications in Signal and Image Processing III*, Proc. SPIE 2569 (1995) 68–79.
- 15 [7] B. Weber, T. Malina, K. Menne, A. Folkers, V. Metzler, U.G. Hofmann, Handling large files of multisite microelectrode recordings for the European VSAMUEL consortium. *Neurocomputing*, June 2001.
- 17 [8] M.V. Wickerhauser, in: *Adapted Wavelet Analysis from Theory to Software*, A K Peters, Wellesley, MA, 1994.
- 19
- 21



**Andre Folkers** has studied Computer Science with emphasis on Medical Computer Science at the Medical University of Lübeck from 1994 until 2000, where he graduated with the Dipl.-Inform. degree, having performed his diploma thesis at the University of Maryland at College Park. Since 2000 he is research assistant in the Institute for Signal Processing at the Medical University of Lübeck working in the project VSAMUEL. His main research interests are advanced biosignal processing, image processing and databases, and multichannel analysis.



**Florian Mösch** joined the project VSAMUEL in 2001 as a student of Computer Science of the Medical University of Lübeck. He graduated with the Dipl.-Inform. degree in 2002, having performed his diploma thesis on the development of a multichannel data acquisition system. Currently he is working in the Institute of Signal Processing at the Medical University of Lübeck. His research fields include multichannel data acquisition and biosignal and image processing.



**Thomas Malina** studies Computer Science at the Medical University of Lübeck since 1995. He was born 1974 in Teschen/Poland and joined the VSAMUEL project in 1999. His research interests are image and signal processing, in particular spike sorting, 3D-modelling and cluster analysis. He was an exchange student at the Aalborg Universitet in Denmark where he developed a data acquisition system. Currently he is working on his diploma thesis at the Medical University of Lübeck.



**Ulrich G. Hofmann** received his Diploma in Physics 1993 and his Ph.D. in Biophysics 1996 from the Technical University of Munich, Germany. He stayed at the Abo Akademi, Finland, as an EU-fellow (HCM) and as Feodor-Lynen-Fellow at the California Institute of Technology. Since 1999 he is research assistant (“Habilitation”) at the Institute for Signal Processing of the Medical University of Lübeck and project coordinator and initiator of VSAMUEL. His long term research aims to interface brains with computers.

3  
5  
7  
9  
1

UNCORRECTED PROOF